

Halo millisecond pulsars ejected by intermediate mass black holes in globular clusters

A. Sesana¹, N. Sartore², B. Devecchi³, A. Possenti⁴

¹*Albert Einstein Institut, Am Mühlenberg 1, Golm, D-14476, Germany.*

²*INAF - Istituto di Fisica Spaziale e Fisica Cosmica, via E. Bassini 15, I-20133 Milano, Italy.*

³*Leiden Observatory, Niels Bohrweg 2, NL-2333 CA, Leiden, The Netherlands.*

⁴*INAF - Osservatorio Astronomico di Cagliari, Loc. Poggio dei Pini, Strada 54 - 09012 Capoterra (CA), Italy.*

Received —

ABSTRACT

Intermediate mass black holes (IMBHs) are among the most elusive objects in contemporary astrophysics. Both theoretical and observational evidence of their existence is subject of debate. Conversely, both theory and observations confirm the presence of a large population of millisecond pulsars (MSPs) with low mass companions residing in globular cluster (GC) centers. If IMBHs are common in GC centers as well, then dynamical interactions will inevitably break up many of these binaries, causing the ejection of several fast MSPs in the Galactic halo. Such population of fast halo MSPs, hard to produce with ‘standard’ MSP generation mechanisms, would provide a strong, albeit indirect, evidence of the presence of a substantial population of IMBHs in GCs. In this paper we study in detail the dynamical formation and evolution of such fast MSPs population, highlighting the relevant observational properties and assessing detection prospects with forthcoming radio surveys.

Key words: black hole physics – stars: kinematics – pulsars: general – globular clusters: general – techniques: radar astronomy

1 INTRODUCTION

Black holes (BHs), with masses ranging from tens to billion solar masses, are among the most exciting objects in the astrophysical world. Although there is nowadays plenty of evidence for the existence of stellar mass BHs ($M \sim 10 M_{\odot}$) and massive BHs (MBHs, $M > 10^6 M_{\odot}$), there is no convincing observational proof for the existence of BHs in the $100 M_{\odot}$ - $10^5 M_{\odot}$ range, the so called intermediate mass BHs (IMBHs). IMBHs could form as a result of dynamical instabilities in dense stellar clusters. Despite the large number of works devoted to this problem, any firm conclusion is still lacking. Runaway collisions between massive stars after their sinking into the cluster center provides a channel to form a very massive ($\sim 10^3 M_{\odot}$) star in the center. This object would be expected to collapse into an intermediate mass black hole (Miller & Hamilton 2002; Portegies Zwart & McMillan 2002; Portegies Zwart et al. 2004) retaining most of the progenitor mass. More detailed simulations including stellar evolution and feedback from stellar winds at solar metallicities, show a systematic inefficiency in growing the central object to masses larger than $\sim 100 M_{\odot}$ (e.g., Glebbeek et al. 2009). IMBHs could then form only in those initially metal poor systems for which stellar mass loss via stellar wind would be strongly reduced.

If theoretical results are unclear, observational evi-

dences are at best elusive. Globular clusters (GCs), among the densest stellar systems known in galaxies, have become prime sites for IMBH searches. The presence of an IMBH would affect the dynamics of the cluster in several ways, and in the last decade many signatures have been proposed. The presence of an IMBH would ‘heat’ the stellar density profile, creating a large core (Baumgardt et al. 2005; Trenti 2008; Umbreit et al. 2009). Therefore, IMBHs are likely to reside in those cluster showing a large r_c/r_h ratio, where r_c and r_h are the core and the half light radii, respectively. Observations suggest (Baumgardt et al. 2005) that this may be the case for $\sim 30\%$ of the Milky Way (MW) GCs. Another clear fingerprint is the Keplerian rising of the velocity dispersion of the stellar distribution inside the sphere of influence of the IMBH. However, for typical IMBH masses, such signature would appear on sub-arcsecond scales, at the limit of current optical facilities. Ibata et al. (2009) report the detection of a Keplerian cusp in M54, consistent with a central $10^4 M_{\odot}$ IMBH (although radial anisotropy in the stellar distribution may explain the observations as well). Several other line-of-sight velocity studies were undertaken by Baumgardt et al. (2003a), van den Bosch et al. (2006), and Chakrabarty (2006) on M15, by Gebhardt et al. (2002), Baumgardt et al. (2003b), Gebhardt et al. (2005) on G1, by Noyola et al. (2008), Sollima et al. (2009), van der Marel &

Anderson (2010) on Omega Centauri, resulting for now in no undisputed definitive detection. Globular clusters are old systems with relaxation timescales shorter than their lifetimes. The most massive stars should then have had enough time to segregate into the center via dynamical friction. This mass segregation should be partially suppressed by the presence of an IMBH. Several studies on the radial dependence of the stellar mass function in different cluster might be consistent with the presence of an IMBH (see Beccari et al. 2010 for M10, Pasquato et al. 2009 for NGC 2298, Umbreit et al. 2009 for NGC5694). However, the presence of primordial binaries can mimic the same effect of an IMBH, and it is not clear to what extent the results depend on the chosen initial conditions. Lastly, an IMBH would accrete ambient gas, and such accretion activity may be observable in X-ray and/or radio. Measurements of radio luminosity of few Galactic GCs put stringent upper limits on IMBH masses (Maccarone & Servillat 2008). Similarly, Cseh et al. (2010) impose a limit of $1500 M_{\odot}$ to any putative massive object in the center of NGC 6388, by using combined X-ray and radio observations. We notice, however, that these limits are affected by a number of parameters (like the accretion efficiency, the gas content in GCs, etc.) that are not constrained themselves.

Millisecond pulsars (MSPs) are usually associated with dense stellar environment, as their formation channel requires a recycling phase within a binary (Camilo & Rasio 2006, Lorimer 2008): almost two thirds (140 out of 220) of the known MSPs are observed in GCs, most of them in binary systems residing in the GC cores (Lorimer 2008). The simultaneous presence of an IMBH and of MSPs in binary systems in the same GC opens interesting dynamical possibilities. Dynamical interactions with an IMBH are expected to break-up binaries ejecting one of the components while leaving the other one bound to the IMBH (Hills 1988, see Devecchi et al. 2007 in the context of IMBHs). One consequence of the presence of IMBHs in GCs would then be the presence of a halo population of fast MSPs, ejected by this tidal break-up process. The detection of such population of fast halo MSPs would not provide a direct evidence for the presence of an IMBH in any particular cluster, but will prove the existence of a population of IMBHs residing in GCs and capable of ejecting MSPs via dynamical interactions. In this paper, we investigate the properties of the expected fast halo MSP population for a range of formation models, assessing observability with forthcoming radio instruments, such as the Square Kilometre Array (SKA, Lazio 2009).

The paper is organized as follows. In Section 2 we introduce the main ingredients of our models, namely the GC IMBH and MSP populations. The binary-IMBH dynamical interaction is detailed in Section 3. In Section 4 we present the population of ejected MSPs highlighting their relevant properties and we discuss observational prospects in Section 5. Our main findings are summarized in Section 6.

2 THE ACTORS ON THE STAGE

2.1 Globular cluster properties

We take the Galactic GC population from the Harris (1996) catalog. We calculate the structural parameters of each GC as follow. We assign each cluster a mass M_{GC} according to

$$M_{GC} = 1.45 \times 10^{(4.8 - M_V)/2.5}, \quad (1)$$

where M_V is the absolute V magnitude given in the catalog, and we used a constant mass to light ratio of 1.45 (McLaughlin 2003) to convert the total cluster luminosity into its mass. We adopt the observed central luminosity and core radius of each cluster listed in the catalog and calculate the central stellar density and the core mass. We provide each cluster with a stellar velocity dispersion according to (McLaughlin 2000)

$$\log \sigma_c = 0.525 \times \log L - 1.928 \quad (2)$$

where L is the total cluster luminosity.

2.2 Intermediate mass black hole populations

We assign each GC a central IMBH assuming two different prescriptions leading to a 'heavy' and a 'light' population of IMBHs. The 'heavy' population ('H' scenario) is obtained using the recipe provided by Portegies Zwart (2005) for the runaway collision formation of an IMBH in a dense stellar cluster. The forming IMBH mass can be written as:

$$M \simeq m_{\text{seed}} + 4 \times 10^{-3} f_c M_{GC} \ln \Lambda. \quad (3)$$

Here $m_{\text{seed}} = 50 M_{\odot}$ is the mass of the heavy star that initiates the runaway process, $\ln \Lambda = 10$ is the Coulomb logarithm and $f_c = 0.2$ is a runaway efficiency factor. As shown in figure 1, this prescription leads to a typical IMBH mass of the order of $10^{-2} M_{GC}$. The recipe given by equation (3) is appropriate in the context of IMBH formation in young dense star clusters, where the core relaxation time is shorter than the lifetime of the most massive stars ($\sim 3\text{Myr}$). This is not the case for GCs in the MW, which have core relaxation times $> 10^7\text{yrs}$, even though they may have suffered a significant core expansion during their life (Binney & Tremaine 1987). Moreover, predicted IMBHs are quite massive, and some of them are only marginally consistent with upper limits placed by dynamical modelling of observed density and luminosity profiles of few selected GCs (see, e.g., van der Marel & Anderson 2010 for Omega Centauri). As a suitable alternative, we explore the possibility that each cluster hosts an IMBH consistent with a low mass extrapolation of the $M - \sigma$ relation observed in galactic bulges (Tremaine et al. 2002)

$$M_6 = 2\sigma_{70}^4, \quad (4)$$

where M_6 is the BH mass in unit of $10^6 M_{\odot}$ and σ_{70} is the GC velocity dispersion in units of 70 km s^{-1} . Figure 1 shows that this prescription leads to a population of much lighter IMBHs (and we will refer to this prescription as 'L' scenario). In this case we place a lower cut to the IMBH mass: GCs that contain a central IMBH less massive than $30 M_{\odot}$ according to equation (4) are simply considered to be void of a central BH, and do not contribute in the calculation. Note that more than 50% of the galactic GCs do not host an IMBH according to this recipe.

2.3 Millisecond pulsar population

GCs are known to host an exceptionally high number of millisecond pulsars (MSPs). There are 22 MSPs detected in 47 Tucanae (hereinafter 47 Tuc) and more than 30 in Terzan

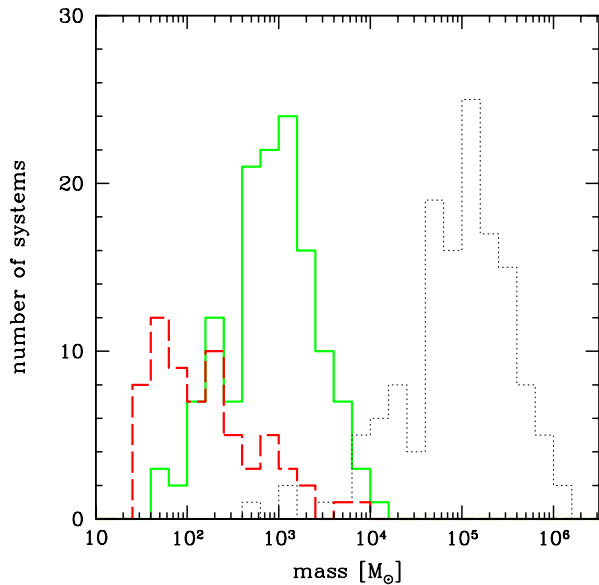


Figure 1. Dotted black histogram: distribution of GC masses (calculated using the Harris 1996 catalog). For each cluster we assign an IMBH with mass given by extrapolating the $M - \sigma$ relation (Tremaine et. al 2002, long-dashed red histogram), or by using a recipe proposed by Portegies Zwart (2005) for the formation of an IMBH in a young dense star cluster (solid green histogram).

5. There is, up to date, a total of ~ 140 MSPs discovered in more than 20 GCs¹, the majority of them being in tight binary systems. It is worth to notice that ongoing surveys are only sensitive to the brightest pulsars hosted in nearby GCs. It is therefore possible that many more pulsars than the $\sim 20 - 30$ currently detected are hosted by massive GCs like 47 Tuc and Terzan 5. Dynamical modeling of dense clusters shows that dense massive clusters in the MW can host as many as 500 MSPs (see detailed discussion in Ivanova et al. 2008a). Assuming that 20 – 40% of the MSPs are observable because of beaming (Kramer et al. 1998; Lorimer 2008 and references therein), this implies $\sim 100 - 200$ observable MSP might be hosted by such clusters, the vast majority of them being below our current detection threshold (Camilo & Rasio 2005). The number of potentially observable MSPs in 47 Tuc estimated by Camilo et al. (2000) by extrapolating the observed MSPs luminosity function to the faint end is in fact ≈ 200 . Note, however, that measurements of the integrated unresolved radio flux from 47 Tuc suggest that the faint undetected population might be of the order of just $\lesssim 30$ objects (McConnell et al. 2004). Interestingly, more than half of the observed MSPs are in binary systems, and are concentrated in the GC cores. Assuming a close correlation between low-mass X-ray binaries (LMXBs) and the MSP formation (van den Heuvel & van Paradijs 1988), as supported by the recent observation of a MSP binary with a shut-off accretion disk (Archibald et al. 2009), we populate each cluster with a number of MSPs in binaries scaling as:

¹ an updated catalog is available at <http://www.naic.edu/~pfreire/GCpsr.html>

$$N_{\text{MSP}} \propto \left(\frac{\rho_0^2 r_c^3}{\sigma_c} \right)^{0.74}, \quad (5)$$

which is approximately the observed scaling between the number of LMXBs and the GC structural parameters (Pooley et al. 2003)²: the central density ρ_0 , the core size r_c and the velocity dispersion σ_c . The term in parenthesis simply describes the formation rate of close binaries in a dense environment: this is proportional to the squared object density multiplied by the volume and divided by the typical relative velocity between objects. As a study case we normalize equation (5) to 50 potentially observable (i.e., beamed toward the Earth, irrespectively of their luminosity) MSPs in binaries in the core of 47 Tuc. All our results can be re-normalized by changing this number.

3 MODELLING THE IMBH-BINARY INTERACTION

A large population of MSPs in binaries would be affected by the presence of an IMBH in the GC center. Close interactions between the binary and the IMBH would cause the tidal break-up of the binary, with one of the two members being ejected from the cluster with high speed and the other being captured in a very eccentric orbit (Hills 1975, Hills 1988, Bromley et al 2006, Sesana Haardt & Madau 2007).

3.1 The tidal disruption cross section

Let us start by modelling the dynamical interactions of a massive object embedded in a population of light field binaries. The target is an IMBH of mass M and the bullets are binaries containing a MSP of mass $m_1 = 1.4 M_\odot$ and a lighter companion of mass m_2 . The binary population is specified by a semimajor axis distribution a_b , by the binary center of mass velocity with respect to the IMBH v_b , and by the mass of the companion to the MSP m_2 . We denote the binary semimajor axis probability distribution by $g(a_b)$. This distribution is derived by fitting the data presented by Camilo & Rasio (2005). Observations show a bimodal binary population, characterized by half of the MSPs having a very light ($m_2 \sim 0.03 M_\odot$) and very close ($a_b < 0.01$ AU) companion, and the other half being accompanied by heavier stars ($m_2 \sim 0.1 - 0.3 M_\odot$) in wider orbits ($a_b \sim 0.02$ AU, with a long tail extending to 0.2 AU). We fit such distribution by (i) an asymmetric Landau profile, peaked at 0.005 AU, in the range [0.0024 AU, 0.02 AU], plus (ii) a Gaussian profile, centered around 0.026 AU, in the range [0.02 AU, 0.035 AU]. We denote the center of mass velocity distribution as $f(v)$ and we assume it follows a Maxwellian distribution with 1-D dispersion σ_c . As we will see below, only the total mass $m_1 + m_2$ enters in the derivation of the cross section and the interaction rate, and since $m_2 \ll m_1$,

² Note that our assumption has a double source of uncertainty. Firstly, the relation expressed in equation (5) has a large scatter, and secondly the relation is for LMXB and not for MSPs. For example, according to equation (5) one would expect several MSPs in NGC 6388, where ≈ 10 LMXB have been detected by Chandra (Nucita et al. 2008); however, none has been found to date.

we will neglect the m_2 dependence in their computation. The m_2 distribution is instead consistently sampled in the evaluation of the ejection velocity, which crucially depends on the mass of the MSP companion (Section 2.3).

The relevant lengthscale for computing the break-up cross section and a relative rate is then the tidal break-up radius, defined as

$$r_{\text{tb}} = \left(\frac{M}{m_1 + m_2} \right)^{1/3} a_b, \quad (6)$$

We consider a close interaction to be efficient when it leads to the break-up of the binary. In this respect, r_{tb} does not mark a clear distinction between tidal break-up and binary survival, but there is a smooth transition between the two regimes around r_{tb} , described by a break-up probability function (Hills 1975)

$$p_{\text{tb}}(r_m/a_b) = 1 - \frac{D}{175}, \quad (7)$$

$$D = \frac{r_m}{a_b} \left[\frac{2M}{10^6(m_1 + m_2)} \right]^{-1/3}. \quad (8)$$

Here r_m is the closest approach of the binary center of mass to the IMBH. When $r_m = r_{\text{tb}}$, $p_{\text{tb}} \sim 0.5$, and it smoothly approaches zero for $r_m \gg r_{\text{tb}}$. To model the ejection rate of MSPs, we need to define an interaction cross section, and an ejection timescale. In general the interaction rate for an IMBH embedded in a background of field objects with number density n and 1-D velocity dispersion σ_c is given by:

$$\Gamma = n \sqrt{3} \sigma_c \Sigma, \quad (9)$$

and the cross section Σ is formally defined as an integral over the impact parameters b

$$\Sigma = 2\pi \int_0^{b_{\text{max}}} b db. \quad (10)$$

Any given impact parameter is related to the closest approach r_m to the IMBH by:

$$b^2 \simeq \frac{2GM r_m}{v_b^2}, \quad (11)$$

where we assumed (as it is always the case for our systems) that the cross section is dominated by gravitational focusing. The range of r_m leading to a disruption depends on a_b , and the focusing depends on v_b . We then define an effective cross section taking into account for the distributions $g(a_b)$, $f(v)$ and for the disruption probability $p_{\text{tb}}(r_m/a_b)$ by writing:

$$\Sigma = \frac{4\pi GM \int dv f(v) v_b^{-2} \int da_b g(a_b) \int dr_m r_m p_{\text{tb}}(r_m/a_b)}{\int dv f(v) \int da_b g(a_b)}. \quad (12)$$

Finally, equation (9) can also be rewritten as

$$\Gamma = n \sqrt{3} \sigma_c \Sigma = N \frac{\sqrt{3} \sigma_c \Sigma}{V_c} = \frac{N}{\tau}, \quad (13)$$

defining a characteristic interaction timescale $\tau = V_c/(\sqrt{3} \sigma_c \Sigma)$. Here V_c is the volume of the GC core, computed via $V_c = (4/3)\pi r_c^3$, using the values of r_c found in the Harris catalog. We consider the volume of the core because most of the MSPs are found in cluster cores, we then assume this is the volume scale relevant for setting the dynamical timescale of the process.

3.2 Consistent evolution of the MSP population

We now consider the population of globular clusters given by the Harris catalog, labelled by the index $i = 1, \dots, 146$. We explore two models for the dynamical evolution of the binaries containing a MSP in GCs. In both scenarios we assume that N_0^i *potentially observable* (i.e., with radio emission beamed toward the Earth) MSPs in binary systems are produced in each GC over its lifetime, starting from $t_0 = -12$ Gyr up to now. In model I we consider that all the N_0^i systems were formed in a single burst at t_0 . In this case, the evolution of the binary population in each individual GC is simply dictated by the tidal break-up rate, and it is described by an exponential decay:

$$N^i(t) = N_0^i e^{-t/\tau^i} \quad (14)$$

(τ^i is the interaction timescale, as defined by equation (13), which is different for each cluster). The binary disruption rate is

$$\Gamma^i(t) = \frac{N_0^i}{\tau^i} e^{-t/\tau^i}, \quad (15)$$

and the number of disrupted systems in 12 Gyr is:

$$N_{\text{ej}}^i = \int_{t_0}^0 \frac{\Gamma^i(t)}{2} dt = N_0^i (1 - e^{-t_0/\tau^i}). \quad (16)$$

Note the factor 1/2 in equation (16). This is because following the tidal break-up, one of the two component of the binary is indifferently ejected (Sari Kobayashi & Rossi 2010, Kobayashi et al. 2012). It is therefore reasonable to expect that only $\sim 50\%$ of the interacting MSP will be ejected. Given a total number of binaries N_0^i , if the number of ejected MSPs is N_{ej}^i , the number of MSPs retained in binaries is $N_{\text{ret}}^i = N_0^i - 2N_{\text{ej}}^i$. (Note that MSPs that remain bound to the IMBH have characteristic coalescence timescales that are $\lesssim 10^8$ yr (Devecchi et al. 2007). Formed IMBH-MSP binaries are thus expected to coalesce before the next interaction of the IMBH with another binary containing an MSP.)

In model II we assume that the N_0^i MSPs are formed at a constant rate from t_0 to now. The evolution of the population is then described by a constant formation rate term plus a loss term dependent on the break-up rate. The solution is given by:

$$N^i(t) = \frac{N_0^i}{t_0} \tau^i (1 - e^{-t/\tau^i}). \quad (17)$$

The binary disruption rate is

$$\Gamma^i(t) = \frac{N_0^i}{t_0} (1 - e^{-t/\tau^i}), \quad (18)$$

and the number of disrupted systems in 12 Gyr is:

$$N_{\text{ej}}^i = \int_{t_0}^0 \frac{\Gamma^i(t)}{2} dt = N_0^i \left[1 - \frac{\tau^i}{t_0} (1 - e^{-t_0/\tau^i}) \right]. \quad (19)$$

Each model provides a consistent way to calculate the total MSP ejections from each single cluster and the rate at which the break-ups occur. The total number of formed, ejected and retained MSPs are simply computed by summing over the GC population: $N_0 = \sum_{i=1}^{146} N_0^i$; $N_{\text{ej}} = \sum_{i=1}^{146} N_{\text{ej}}^i$; $N_{\text{ret}} = \sum_{i=1}^{146} N_{\text{ret}}^i$. MSP ejection rates for all our four models (H-I, H-II, L-I, L-II) are shown in figure 2, which highlights the completely different ejection histories of the two scenarios.

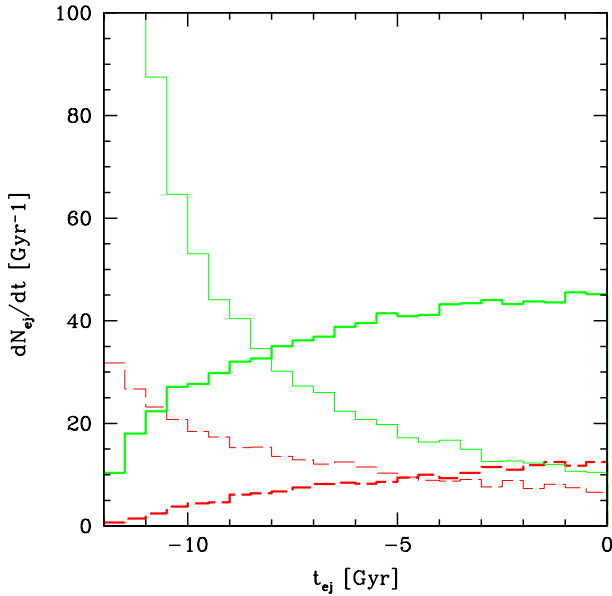


Figure 2. MSPs ejection rates for our four models. The H models (from here on) are shown with solid green lines and the L models (from here on) are shown with long-dashed red lines. Thin lines are for the MSP formation scenario I (formation burst at t_0) and thick lines are for the MSP formation scenario II (constant formation rate from t_0 to now).

In models I, the rate follows a simple exponential decay (it is actually a sum of exponential decays because each GC has its peculiar interaction timescale τ^i). In models II, instead, the ejection rate is initially limited by the availability of binaries, and it is a monotonic increasing function of time.

3.3 Ejection velocity

After the break-up, one of the binary components is ejected with mean velocity

$$v_{ej} \simeq 1430 a_{b,0.01}^{-1/2} (m_1 + m_2)_0^{1/3} M_3^{1/6} f_R \text{ km s}^{-1}, \quad (20)$$

where $a_{b,0.01}$ is the binary semimajor axis in units of 0.01 AU, $(m_1 + m_2)_0$ is the binary mass in units of $1 M_\odot$ and M_3 is the IMBH mass in units of $10^3 M_\odot$. The factor f_R , of order unity, is fitted against numerical simulation and takes the form (Bromley et al. 2006)

$$f_R = 0.774 + (0.0204 + (-6.23 \times 10^{-4} + (7.62 \times 10^{-6} + (-4.24 \times 10^{-8} + 8.62 \times 10^{-11} D)D)D)D, \quad (21)$$

where D is defined by equation (8). For any given combination of the parameters (a_b , $m_1 + m_2$, M), the distribution of ejected velocities is well approximated by a Gaussian with mean value v_{ej} and dispersion $0.2v_{ej}$. The mean ejection velocity of the primary is $v_{ej,1} = [2m_2/(m_1 + m_2)]^{1/2} v_{ej}$, and that of the secondary is $v_{ej,2} = [2m_1/(m_1 + m_2)]^{1/2} v_{ej}$. Binary MSPs are usually found in systems with $m_2/m_1 \lesssim 0.2$, so that their typical ejection velocity is of the order of $300 - 400 \text{ km s}^{-1}$. Ejection velocity distributions are shown in figure 3 for all our models. In all the cases, the distribution is bimodal, reflecting the bimodality in the semimajor axis and companion mass distributions highlighted by

Camilo & Rasio (2005). L models produce a flat velocity distribution in the range $100-500 \text{ km s}^{-1}$, while H models are strongly peaked around 500 km s^{-1} . These values are interesting because most of the MSPs will be able to travel far in the halo remaining bound to the Galaxy: even though the global ejection rates are $< 10^{-7} \text{ yr}^{-1}$, we may expect an accumulation of several hundreds of fast halo MSPs during the MW lifetime. As a possible contaminant population, we consider a putative distribution of pulsars ejected by the Galactic center. Since little is known about neutron stars and MSPs in the Galactic center, we decided to model it by adopting the same prescriptions as for GCs. The number of MSPs in binaries is derived according to equation (5) where we used the following parameters: $r_c = 2.2 \text{ pc}$, $\sigma_c = 100 \text{ km s}^{-1}$, $\rho_0 = 8 \times 10^6 / (4/3\pi r_c^3) M_\odot \text{ pc}^{-3}$. The mass of the MBH is assumed to be $M = 4 \times 10^6 M_\odot$ (Gillessen et al. 2009). As shown in figure 3, ejection velocities are in this case usually higher than 800 km s^{-1} (primarily because the MBH in the Galactic center is much more massive than the putative IMBHs populating GCs), implying that most of them will escape the MW halo, and we may expect only and handful of contaminant fast MSPs coming from the Galactic center. Note that according to this simple model $\gtrsim 1000$ binary MSPs are produced within 2.2pc from Sgr A* over an Hubble time. By comparison, X-ray counts published by Muno et al. (2003), imply ~ 1000 hard X-ray sources within 20 pc from Sgr A*. As the detected space density approximately increases as the inverse square of the distance, we infer ~ 100 X-ray sources within 2 pc from Sgr A*. However, only a small fraction \mathcal{F} of them are expected to be MSP progenitor X-ray binaries. This implies a number of MSPs forming in binaries within 2.2pc around Sgr A* in an Hubble time T_H of the order of $100\mathcal{F}T_H/T_X$; which is less than the fiducial number we use, as long as the average lifetime of a MSP progenitor X-ray binary is $T_X \gtrsim \mathcal{F}10^9 \text{ yr}$. We conclude that the oversimplistic scenario adopted here for the Galactic center provides a reasonable estimate of the resulting MSP contaminant population (we will further discuss contaminant populations in Section 4.3).

We should notice, at this point, that our ejected MSP population models (rates and velocities) are derived from the MSP binary population *observed today*. However, MSP binaries might have suffered significant dynamical interactions with other stars and binaries in the dense environment of GC cores. The typical binary-single star encounter timescale is given by (King et al. 2003)

$$\tau_{enc} = 7 \times 10^{10} \text{ yr } \sigma_{10} n_5^{-1} R_m^{-1} M^{-1}, \quad (22)$$

where n_c is the core number density in units of 10^5 pc^{-3} , σ is the velocity dispersion in units of 10 km s^{-1} , and R_m and M are the maximum encounter approach and the total mass of the three bodies in solar radii and solar masses respectively. For typical observed MSP binaries and dense cluster parameters, the timescale for an encounter at $R_m \sim a$ is $\sim 10^{10} \text{ yr}$. Hence, only perhaps few strong encounters might have occurred since their formation. However, strong interactions certainly play a role in the MSP population evolution, otherwise we would not see isolated MSPs in GCs (whereas, in fact, 40% of them are, Lorimer 2008). Such interactions are neglected in the evolutionary models presented here. Their main result is to change the binary semimajor axis a and the companion mass m_2 (in an exchange encounter), there-

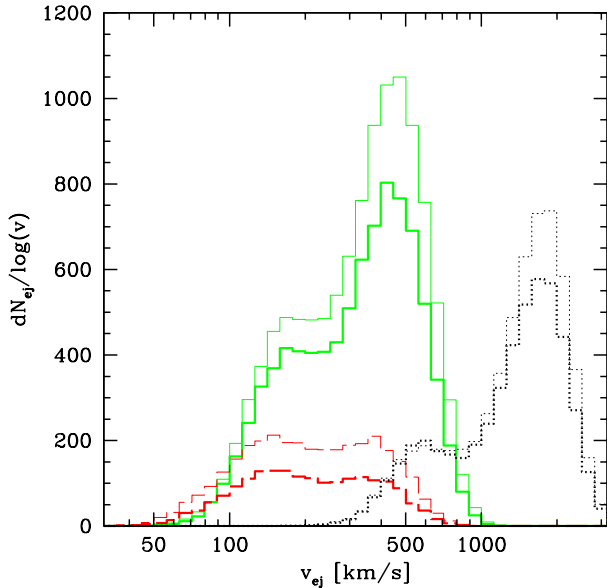


Figure 3. Velocity distribution of ejected MSPs. Linestyle as in figure 2 for the four models H-I, H-II, L-I, L-II. The dotted histograms are for a putative contaminant population of ejected MSPs from the Galactic center. Thin and thick histograms correspond to scenarios I and II for the MSP formation.

fore affecting the subsequent MSP binary interaction cross section with the IMBH (wider binaries are easily disrupted). On the other hand, the ejection velocity is only mildly dependent on a and m_2 (see equation (20)). As an extreme case, we tested a scenario where all the MSP companions have $m_2 = 0.5 M_\odot$ and the a distribution is three times wider than that described in Section 3.2. The net result is a $\gtrsim 50\%$ increase in the number of ejections with a $\sim 25\%$ decrease in the typical ejection velocity. We therefore conclude that evolution of the MSP binary population will affect our results within a factor less than two, much smaller than the impact of changing the IMBH population (see red vs. green curves in figure 3).

3.4 Composing the puzzle

We assign to each GC an IMBH according to one of the prescriptions given by equations (3) and (4). We then compute Σ^i for each GC (equation (12)) and the interaction timescale τ^i , assuming a population of MSPs described by a distribution of semimajor axis $g(a_b)$ and of velocity at infinity $f(v)$. These numbers are then plugged into equations (16) and (19) to compute how many binaries are ejected according to the two different MSP formation scenarios. To do so, N_0^i is set to 50 in 47 Tuc, and it is scaled to other GCs according to equation (5). We then generate a Monte Carlo population of binaries according to $g(a_b)$ and $f(v)$, we target the MBH with a distribution of impact parameter ‘at infinity’ proportional to bdb , and we break-up the binaries according to p_{tb} as given by equation (7). To each disrupted binary we assign a disruption time t_{ej} drawn from a probability distribution proportional to the rates (15) and (18), and we assign a ve-

locity v_{ej} according to the procedure described in Section 2.3 (equation (20)).

MSPs are then ejected from GCs, or the Galactic center, and their orbits are integrated in the MW potential with the PSYCO³ code (Sartore et al. 2010). Orbit integration is carried out in the following way: for MSPs ejected from GCs, we first initialize the orbit of each GC. The initial positions of GCs are taken from the Harris catalog, while we assign a random velocity taken from a Gaussian distribution with dispersion (Brown et al. 2010)

$$\sigma = 116 - 0.38 \times r \text{ km s}^{-1}, \quad (23)$$

where r is the distance from the Galactic center in kpc. We then follow the orbit of the i -th GC for 12 Gyrs and store its position \mathbf{r}_{GC}^i and velocity \mathbf{v}_{GC}^i at each disruption time. At this point we initialize the orbit of each MSP, its initial position and velocity being $\mathbf{r}_{\text{MSP}} = \mathbf{r}_{\text{GC}}(t_{\text{ej}})$ and $\mathbf{v}_{\text{MSP}} = \mathbf{v}_{\text{GC}}(t_{\text{ej}}) + \mathbf{v}_{\text{ej}}$, respectively. Both positions and velocities are defined in a Galactocentric cylindrical frame (R, ϕ, z) and the direction of \mathbf{v}_{ej} is random. In the case of MSPs ejected from the Galactic center, these are initially placed at $r = 2$ pc ($\sim r_c$) from the MBH, while now $\mathbf{v}_{\text{MSP}} = \mathbf{v}_{\text{ej}}$ and is assumed to be purely radial⁴.

4 RESULTS

4.1 Population of ejected and retained MSPs

In figure 4 we show the distribution of the fraction of MSPs ejected by each GC. Only clusters forming at least one MSP according to equation (5) are shown. In the L scenario, the vast majority of the clusters retain all the MSPs because there is no IMBH in their center, or the IMBH mass is so small that its tidal break-up cross section is negligible. Only ~ 20 GCs eject a significant fraction of their MSPs. In the H scenario still $\sim 30\%$ of the clusters retain all their MSPs, but several of them eject a significant fraction of systems. Note that here we plot the fraction of *ejected* MSP, and only 50% of the disrupted binaries result in the MSP ejection. A fraction of ejected pulsars of 0.5 then means that the IMBH has disrupted all the binaries hosting MSPs, and the other 0.5 fraction of MSPs remained bound to the IMBH. This scenario is consistent with results of 3-body simulations (Devecchi et al. 2007). Further evolution of newly formed IMBH–MSP binaries is dictated by i) hardening due to three body interactions with other cluster stars and ii) gravitational wave emission. These two processes generally lead to a rapid coalescence ($\sim 10^8$ yr) of the binaries.

The contribution of each GC to the ejected population of MSPs is shown in figure 5. If the IMBH mass is assigned according to the $M - \sigma$ relation, then only ~ 20 GCs contribute to the halo MSP population ejecting at least one object. Interestingly, BHs with masses as low as $100 M_\odot$ can eject ~ 10 MSPs during an Hubble time. In the H scenario, ~ 50 GCs eject at least 1 MSP. The total numbers of ejected

³ Population SYnthesis of Compact Objects

⁴ We consider purely radial velocities because the tidal break-up radius for a typical binary orbiting Sgr A* is of the order of mpc, much smaller than the initial radius of orbit integration ($r = 2$ pc).

MODEL	N_0	N_{ret}	N_{ej}	$N_{\text{ej,obs}}(\mathcal{A})$	$N_{\text{ej,obs}}(\mathcal{B})$
H-I	1929	789	570	64	18
H-II	1929	1047	441	50	11
L-I	1929	1597	166	25	6
L-II	1929	1706	103	14	3

Table 1. MSPs in the four different models (first column). We show the total numbers of produced MSPs in binary systems (N_0 , column 2), the number of retained MSPs following binary disruption (N_{ret} , column 3), and the number of ejected ones (N_{ej} , column 4). Columns 5 and 6 are the number of MSPs ejected by IMBHs residing in GCs into the MW halo that will be detectable with SKA in configuration \mathcal{A} and \mathcal{B} , according to simulations described in Section 5.

and retained MSPs are given in table 1. The number of fast MSPs ejected in the halo spans almost an order of magnitude, from ~ 100 (L-II model) to ~ 600 (H-I model), this number can be as high as ~ 1000 if the ejection probability for the MSP is higher than 0.5^5 . The number of retained binaries containing MSPs is instead in the range $800 - 1700$ for the different scenarios. It is therefore very unlikely that a population of IMBHs would completely devoid MSPs in binaries residing in GCs. In the most extreme case, $\sim 50\%$ of the formed binaries are disrupted by scattering with the IMBH. This is because, in general, the characteristic size of the GC core is much larger than the typical disruption cross section Σ , and even assuming that the 'loss cone' is always full (i.e. the nuclear relaxation timescale is much less than the Hubble time, which is always the case for the GC cores), the IMBH does not have enough time to tear apart all the binaries.

As a 'consistency check', we plot in figure 6 the number of surviving MSPs in binaries for each GC. Most of the clusters retain the majority of their MSPs. In particular, even in our H scenario, we find that 47 Tuc would still host ~ 25 observable MSPs in binaries in its core, while ~ 50 retained MSPs are expected in Terzan 5; both numbers are consistent with observations.

4.2 Properties of the ejected MSPs

As stated in the previous section, since MSPs usually have a low mass companion, their typical ejection velocities are not extremely high, and only a small fraction of them has $v > 500 \text{ km s}^{-1}$; thus, they accumulate in the halo basically for an Hubble time, resulting in a consistent population of tens-to-hundreds fast halo MSPs. Therefore, in both H and L scenarios most MSPs remain gravitationally bound to the Galaxy, building up a halo population that extends up to $\sim 100 \text{ kpc}$ from the Galactic center. Typical velocities of these objects are $\sim 200 \text{ km s}^{-1}$, which imply proper motions

⁵ Some author in fact (i.e., Bromley et al. 2006) suggest that in the tidal break-up process, if $m_2 \ll m_1$, then the probability of ejecting the more massive object is substantially higher than 0.5. This is always the case for our systems, since the MSP companion is always a very low mass main sequence star. However, here we preferred to be conservative and assume equal probability for the ejection of the MSP and the low mass companion.

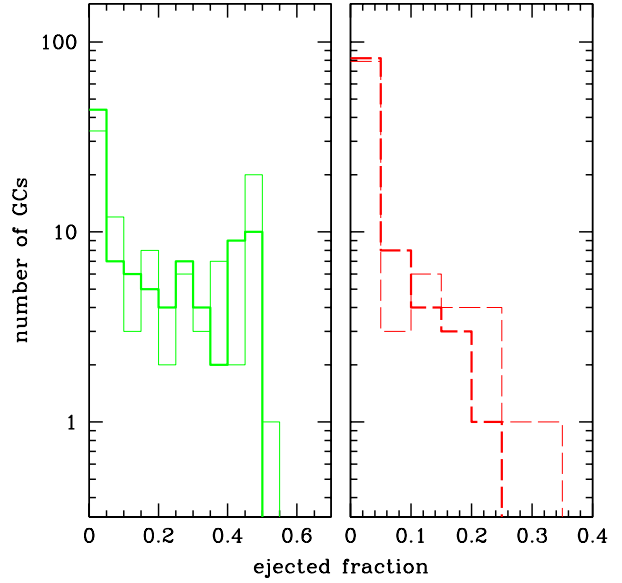


Figure 4. Fraction of ejected MSPs. Left panel: H models; right panels: L models. Note the different scale on the x axis. Thin and thick histograms correspond to scenarios I and II.

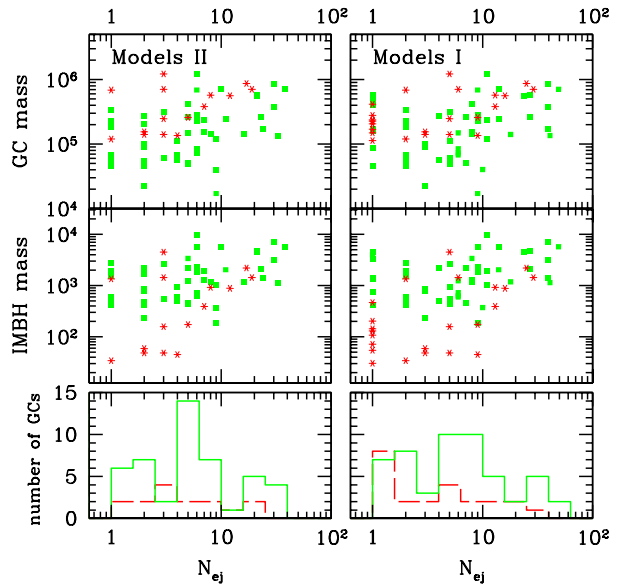


Figure 5. Statistics of ejected MSPs. The different panels represent the number of ejected MSPs versus the mass of the GC (top) and versus the mass of the IMBH (middle), and the distribution of the number of ejected MSPs from each individual cluster (bottom). Left panels are for scenario II and right panels are for scenario I. In each panel, red asterisks are for the L IMBH population model and filled green squares are for the H IMBH population model. In the lower panels, solid green and long-dashed red histograms are for H and L models respectively.

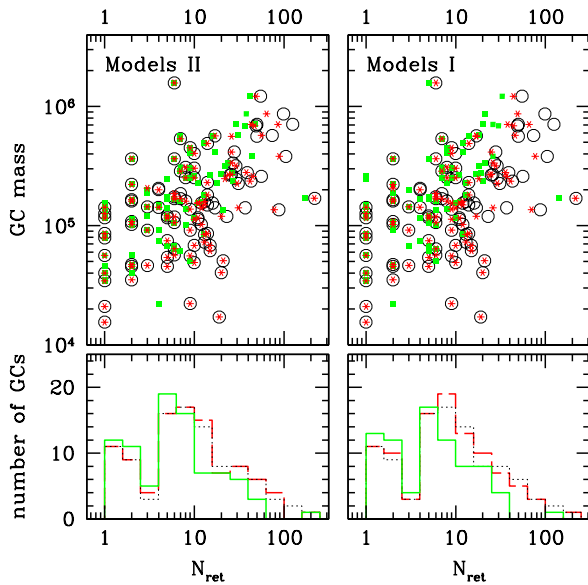


Figure 6. Statistics of retained MSPs. In the top panels we plot the number of MSPs in binaries left in the GCs today versus the mass of the GC, while in the bottom panels we plot the distribution of the number of retained MSPs in each individual cluster. Left panels are for scenario II and right panels are for scenario I. In the top panels, red asterisks are for the L IMBH population model and filled green squares are for the H IMBH population model, while black empty circles mark the total number of generated MSPs in binaries (N_0^i) in each cluster. In the lower panels solid green and long-dashed red histograms are for H and L models respectively; the thin dotted histogram represent the population of generated MSPs.

of $\sim 0.1 - 10 \text{ mas yr}^{-1}$, i.e. well within the capabilities of present and upcoming instruments (especially the SKA). A small fraction of MSPs is in unbound orbits and thus can reach distances of several Mpc.

On the other hand, MSPs ejected from the Galactic center are almost all gravitationally unbound, given the higher ejection velocity induced by Sgr A* compared to the IMBHs. As a consequence, they do not accumulate in the MW halo, travelling at very large radii, up to ~ 10 Mpc. This is particularly important, because it means that such possible ‘contaminant’ population would be essentially undetectable (these MSPs are too far and thus too dim) and can be neglected. For the same reason, hereafter we shall consider the contribution of MSP within $d_{max} \sim 100$ kpc from the Sun.

4.3 Possible sources of contamination

The detection of a fast halo MSP population may provide indirect evidence of IMBHs in GCs. However all possible source of contamination have to be taken into account.

Firstly, the Galactic disk and bulge are known to house ~ 30000 MSPs (Lorimer 2005, Story et al. 2007), born via standard binary evolution channels (Bhattacharya & van den Heuvel 1991). Although by far larger than our predicted fast halo MSP population, there are several considerations that mitigate the contaminant effect of disk MSPs. MSPs are ‘recycled’ objects (van den Heuvel 1995), and are not

affected by strong natal kicks as the ordinary ones. Owing to their unperturbed binary evolution, these MSPs have lower spatial velocities than halo MSPs, with typical transverse velocities of $\sim 80 - 200 \text{ km s}^{-1}$ (e.g. Gonzalez et al. 2011). As a consequence, their spatial distribution is flattened towards the Galactic disk, with scale-height of ~ 0.5 kpc (Story et al. 2007). Moreover, the vast majority of disk MSPs have a binary companion ($\approx 75\%$, Lorimer 2008), whereas the break-up mechanism implies that halo MSPs are all isolated. In any case, given the large disk MSP number, we need to take them into account in simulating observations, in order to quantify the effective separability of the two populations.

Another source of contamination might be due to MSPs released in the halo by cluster evaporation and disruption. It is in fact likely that observed GCs were more massive in the past, undergoing a slow process of dynamical evaporation and tidal stripping (e.g. McLaughlin & Fall 2008). However, MSPs and their massive progenitors are among the heaviest GC objects, and preferentially segregate in the core, rather than being ejected. Following the same line of arguments, a substantial number of GCs might have completely disappeared by now, releasing their stellar content, including putative MSPs, in the halo. However, this release mechanism does not require any strong dynamical interaction, and the MSPs would naturally retain their donors. We also notice that clusters prone to evaporation and disruption are the less dense and massive ones, minimizing (i) the efficiency of MSP production in first place; and (ii) the probability of dynamical interactions depriving the MSPs of their donors. We therefore expect the contamination from halo MSPs produced in completely evaporated clusters to be minor, and mostly composed of MSPs in binary systems.

A further minor contaminant population might come from MSPs directly formed in the halo. The MW halo, in the range 1–40 kpc from the Galactic center, consists of $\sim 3 \times 10^8 M_{\odot}$ of old stars (Bell et al. 2008). Even assuming the same formation rate as in the disk, a population of MSPs directly formed in the halo would count ~ 100 objects. This would be a significant contaminant in our L scenario (see Table 1).

In addition to contaminant populations, we also have to be careful in considering other possible formation channels of fast halo MSPs not requiring IMBHs. The formation of these halo objects must necessarily be dynamical, involving some close interaction with other compact objects. Such dynamical interactions are far too rare in ordinary stellar environment (galactic disk and bulge), and any other formation process must take place in a dense environment, i.e. GCs or the Galactic center. We already discussed the possibility of ejecting MSPs from the Galactic center, and how the resulting population would be significantly different with respect to the one ejected by IMBHs (and, in any case, hardly detectable).

We examine here possibility of ejection following the binary break-up due to binary-single or binary-binary interactions. According to equation (22) MSP binaries might have suffered few strong encounters with single objects in their lifetime. For typical parameters, MSP binaries are extremely hard (i.e., specific binding energy to average GC star specific kinetic energy, $\epsilon_b/\epsilon_k \gg 1$), and the most probable outcomes of a three body interaction are either a flyby with the binary getting harder (unless the intruder is a stellar BH, see

below), or an exchange of companion star: in any case, MSP ejection is very unlikely. Binary-binary interactions are far more complex, and therefore difficult to address. In such encounters the MSP binary is usually the 'harder' in the pair. Therefore, also in this case, it tends to get harder while the other binary gets softer or ionized. The typical interaction outcome is a simple flyby or a breakup of the softer pair (Bacon, Sigurdsson & Davies 1996). Companion exchanges are also possible, whereas individual MSP ejection is unlikely. Close encounters also perturb the MSP binary orbital elements (semimajor axis and eccentricity), possibly leading to the coalescence of the pair. In fact, maybe half of the observed individual binaries in Terzan 5 and 47 Tuc might be the endproduct of dynamically induced mergers (Ivanova et al. 2008a). In this case, no appreciable kick is expected, and the MSP is retained in the cluster. In general, it is likely that individual MSPs will be located approximately where they formed (in cluster cores), with some of them displaced to the cluster halo (Ivanova et al. 2008b). In fact, most of the single MSPs found in clusters are observed in the core, which would be unlikely if the typical outcome of close encounters is ejection at high velocity.

Lastly, MSP binary tidal break-up may occur due to interactions with stellar BHs. The ejection velocity is in fact weakly dependent on the BH mass (see equation 20), meaning that the survival of few stellar BHs in GC centers, may mimic the effect given by IMBHs. However, stellar BHs are thought to segregate efficiently at the center of GCs, forming binaries that interact with each other, resulting in a quick ejection of basically all the stellar BHs from the clusters. Simulations carried by O'Leary et al. (2006) show that basically all the stellar BHs would be ejected in less than a Gyr. We run a test case where we assume a single $10 M_{\odot}$ BH surviving in each cluster. In this case only 10-20 MSPs are ejected, and typical ejection velocities are much lower, in the range $50 - 200 \text{ km s}^{-1}$. Nevertheless, in the unlikely eventuality that all the GCs retain several (> 10) stellar BHs, they would produce a population of ejected MSPs at least comparable to the L model. However, being ejection velocity usually smaller, the resulting MSP distribution would be more concentrated toward the Galactic center, tracing closely the GC distribution in the MW potential.

Therefore, from an observational perspective, the most important contaminant population is that of MSPs born in the Galactic disk through the standard binary evolution channel. Since disk MSPs are much more numerous than halo MSPs, they are likely to dominate the distribution of observed objects, and should be taken into account before claiming the detectability of the fast halo population. In the next chapter we will present a method to characterize halo MSPs and differentiate them from Galactic disk MSPs.

5 THE OBSERVABILITY OF HALO MSPS

The detection of a population of fast isolated halo MSPs would be a strong, albeit indirect, evidence of the existence of IMBHs in GCs. In the previous section we described the properties of such population; we discuss here prospects for its future detection by means of upcoming radio facilities such as the SKA.

5.1 Simulations of the Galactic MSP population

According to Smits et al. (2009), the SKA will potentially detect up to 6000 MSPs from the Galactic disk. This number exceeds that of MSPs which, according to our model, are likely to populate the halo, even in the most favorable case.

Thus, we simulate the radio properties of halo MSPs with the `PSRPOP` code (Lorimer et al. 2006) and compare them with those of Galactic disk MSPs, in order to find an efficient identification method. We assume that both populations have the same intrinsic properties: pseudoluminosity follow a power-law distribution with slope -1 between 0.1 and 100 mJy at 400 MHz (Lyne et al. 1998). Pulse periods are drawn from a lognormal distribution with mean 1 and dispersion 0.2 in units of $\log P$, where P is in milliseconds. Pulse widths are assumed to be 20% of the pulse period. Finally the spatial distribution of disk MSPs is modelled according to Faucher-Giguère and Loeb (2009), with scale-height 0.5 kpc and scale-length 4 kpc, whereas that of halo MSPs is determined by direct orbit integration in the Galactic potential as detailed in Section 3.4. In all runs, we simulate 30000 disk MSPs and a number of halo MSPs taken from Table 1.

We model SKA observations following Smits et al. (2009). Assuming a minimum signal-to-noise (S/N) ratio, then the limit flux density S_{lim} to which the instrument is sensitive can be obtained with the so-called radiometer equation

$$S_{\text{lim}} = \frac{S/N (T_{\text{sys}} + T_{\text{sky}})}{G (n_p t_{\text{obs}} B)^{1/2}} \left(\frac{W}{P - W} \right)^{1/2} \text{ mJy}, \quad (24)$$

where T_{sys} and T_{sky} are respectively the system noise temperature and the sky temperature in Kelvin, G is the telescope gain in K Jy^{-1} , n_p is the number of polarizations, t_{obs} is the integration time in seconds, B is the bandwidth in MHz and P and W are the pulse period and width of the pulsars in seconds respectively. We adopt the following values for the parameters: $T_{\text{sys}} = 30 \text{ K}$, $n_p = 2$, $t_{\text{obs}} = 1800 \text{ s}$, and $B = 512 \text{ MHz}$. For the gain we assume two possible values, relative to two different configurations of the SKA, one with 3000 15m dishes and gain $G \sim 140 \text{ K Jy}^{-1}$ (case \mathcal{A}) and another configuration accounting only the inner core of the array with gain a factor 5 lower (case \mathcal{B}).

The average number of detectable disk MSPs is $\sim 4300^6$ and ~ 1150 for SKA configuration \mathcal{A} and \mathcal{B} respectively. For comparison, detectable halo MSP are always less than 100; numbers for the different models are given in Table 1. For each simulation we store the position and velocity vectors of all detectable MSP, which we use to analyze their observational properties. To smooth the distributions we average over 1000 random realizations of the disk population and 20 full numerical integrations of each halo population (models H-I, H-II, L-I, L-II) in the Galactic potential.

⁶ The difference with the figures quoted by Smits et al. 2009 (i.e. ~ 6000 objects) comes from the different assumptions adopted for the (loosely constrained) disk population. We used the period and luminosity function by Lyne et al. 1998, combined with the spatial distribution by Faucher-Giguère and Loeb (2009), whereas Smits et al. consider a slightly different population model by Cordes and Chernoff (1997).

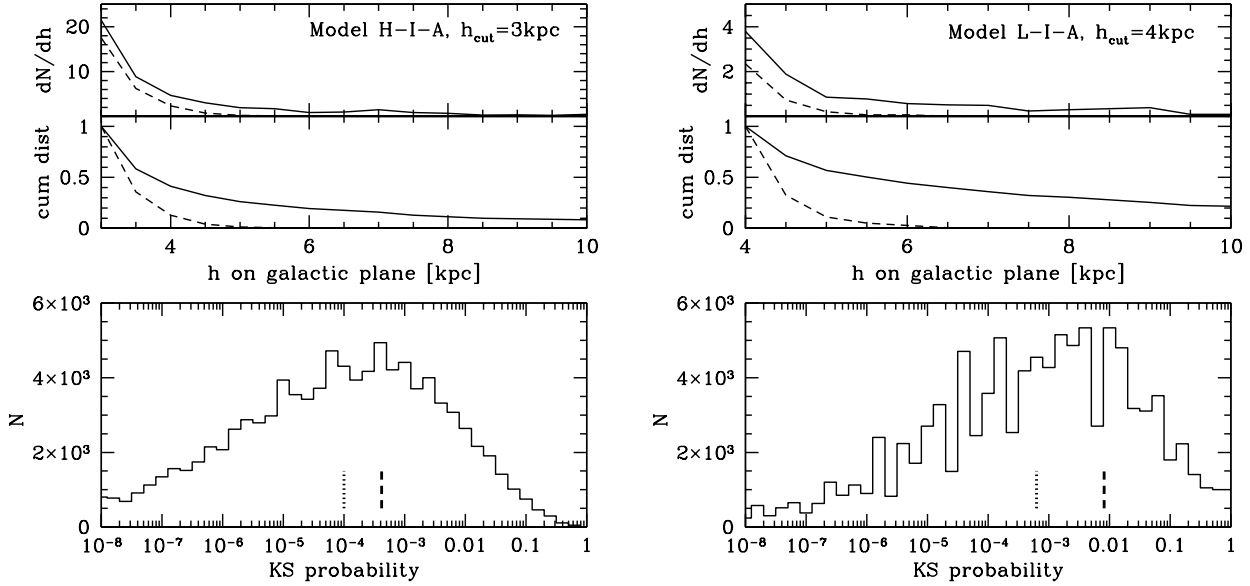


Figure 7. Distribution of observable MSPs and P_{KS} for selected models. In the upper panels we plot the tail of the observed distribution at $h > h_{\text{cut}}$ (top) and the cumulative distribution starting from $h = \infty$ down to h_{cut} . Dashed lines are for the *disk* population and solid lines for the *disk+halo* population. The lower panels show the distribution of P_{KS} that a *disk+halo* Montecarlo sample is erroneously identified as being drawn by the *disk* population only for 10^5 random trials. The vertical ticks represent the mean (dashed) and the median (dotted) of the distributions.

MODEL	$h_{\text{cut}} = 3\text{kpc}$				$h_{\text{cut}} = 4\text{kpc}$			
	N_{disk}	$N_{\text{disk+halo}}$	mean P_{KS}	median P_{KS}	N_{disk}	$N_{\text{disk+halo}}$	mean P_{KS}	median P_{KS}
H-I-A	27.11	51.45	4.31×10^{-4}	10^{-4}	3.47	21.22	9.53×10^{-5}	4.90×10^{-6}
H-II-A	27.11	48.71	2.17×10^{-3}	6.31×10^{-4}	3.47	18.87	6.9×10^{-4}	2.51×10^{-5}
L-I-A	27.11	39.65	3.22×10^{-2}	2.51×10^{-2}	3.47	13.17	7.99×10^{-3}	6.31×10^{-4}
L-II-A	27.11	33.76	0.26	0.25	3.47	8.16	5.52×10^{-2}	1.58×10^{-2}
H-I-B	5.93	12.78	7.47×10^{-2}	3.98×10^{-2}	0.76	5.76	2.66×10^{-2}	1.58×10^{-3}
H-II-B	5.93	12.73	4.55×10^{-2}	1.58×10^{-2}	0.76	6.16	9.50×10^{-3}	2.55×10^{-4}
L-I-B	5.93	10.83	6.59×10^{-2}	1.58×10^{-2}	0.76	5.21	8.04×10^{-3}	1.58×10^{-4}
L-II-B	5.93	10.03	0.17	0.16	0.76	3.81	3.43×10^{-2}	3.98×10^{-3}

Table 2. KS probability for all the eight (four halo MSP generation models times two SKA configurations) investigated scenarios. The first column gives the model label; columns two-to-five give the average number of observable *disk* MSPs, the average number of observable *disk+halo* MSPs and the mean and the median KS probability for 10^5 Montecarlo draws (see text for description) assuming $h_{\text{cut}} = 3$ kpc. Columns five-to-nine give the same quantities for the $h_{\text{cut}} = 4$ kpc case.

5.2 Statistical analysis

With the results of our simulations in hand, we seek for a suitable discriminant between halo and disk objects. Even though the two populations are quite distinct, this is not a trivial task. One obvious discriminant is the binary nature: halo MSPs are isolated, whereas the vast majority of observed disk MSPs (about 75%) are in binaries. However, there are still far more isolated disk MSPs than halo MSPs, and further discriminating properties are necessary. Unlike the case of Hypervelocity stars in the MW halo (Bromley et al. 2006, Sesana et al. 2007), radial velocities cannot be directly measured, and in any case they would be mostly in the range $50\text{--}500 \text{ km s}^{-1}$, providing just a little (if any) discriminant power. Transverse velocities can be measured from the parallax; however, expected values of $0.1\text{--}10 \text{ mas/yr}$ are the same for both populations. Instead of velocity, it turns out

that a better discriminant between the two population is the spatial location of the objects, in particular the distribution of the projected distance h of the MSPs from the disk plane. The good thing about h is that it can be easily measured by SKA. In fact, since MSPs sky locations are known almost exactly, the accuracy in the h measurement is directly related to the measurement of the MSP distance, which for SKA is expected to be better than $\sim 10\%$ at 10 kpc (Smits et al. 2011) thanks to very precise parallax determination. Halo MSPs should reflect the distribution of the parent population of GCs and thus many of them are likely to be found at large distances from the disk. The spatial distribution of disk MSP is instead expected to be extremely flattened in the galactic plane, decaying exponentially at large distances. To quantify this concept, for each GC ejected MSP

population and SKA configuration we extract two distinct distributions:

- the *disk* only distribution of detectable MSPs with disk plane distance $h > h_{\text{cut}}$, with $h_{\text{cut}} = 3, 4, 5$ kpc;
- the *disk+halo* distribution of detectable MSPs, for the same h_{cut} values.

Examples of such distributions are given in the upper panels of figure 7 and numbers are quantified in table 2. The figure highlights that the chance of getting an MSP at $h > 5$ kpc belonging to the *disk* population is almost nil (dashed lines); conversely, when the *disk+halo* population is considered, the distributions show a long tail extending to $h > 10$ (solid lines). This is particularly clear by looking at the normalized cumulative distributions; such distributions are built starting nominally at $h = \infty$, down to a specific value h_{cut} , which, as stated above, we place at 3, 4 and 5 kpc from the galactic plane. The two reported examples highlight the extreme different behavior of the cumulative distributions, which is the starting point of our statistical tests.

The number of MSPs found at large h is already a good indicator of the presence of halo MSPs, as shown in table 2. Here, columns 6 and 7 report the average number of MSPs found at $h > 4$ kpc for the *disk* and the *disk+halo* distribution respectively. The paucity of *disk* pulsars indicates that the detection of a sizable number of MSPs at large h would be a strong hint of a substantial presence of halo MSPs ejected by GCs. To make our analysis more quantitative, we perform, for each ejection model (H-I, H-II, L-I, L-II) SKA configuration (\mathcal{A} , \mathcal{B}) and h_{cut} (3, 4, 5 kpc), a simple Kolmogorov-Smirnov (KS) test on the h distribution predicted by the two populations (*disk* and *disk+halo*). We proceed as follow. We assume that SKA observes a *disk+halo* population of MSPs. To simulate this, we draw a number of observed MSPs, N_{obs} , from a Gaussian distribution with mean value equal to $N_{\text{disk+halo}}$ and variance equal to $\sqrt{N_{\text{disk+halo}}}$; values of $N_{\text{disk+halo}}$ are given in table 2 for the different cases. We then contrast the observed h distribution to that predicted by the *disk* population only and compute the KS indicator P_{KS} . This namely gives the probability that our *disk+halo* drawn sample is erroneously recognized as being drawn from the *disk* only distribution. We repeat the procedure 100000 times. The result depends on the specific sample, and examples of the P_{KS} distribution for two selected models are shown in the bottom panels of figure 7. Even though the P_{KS} distributions have a large dispersion, their mean and median values are usually small, indicating that a characteristic realization of the *disk+halo* distribution can be identified with high confidence. Results of course depend on the underlying halo population and SKA configuration, and also on the adopted value of h_{cut} . If h_{cut} is too small, then the overall distribution is dominated by the disk population, and the large h tail contribution given by halo MSPs becomes marginal, making the KS test ineffective. On the other hand, if h_{cut} is too large, then the number of detectable MSPs is very small, making the test ill defined (at least 4-5 datapoints are needed for a trustworthy KS test). We find an h_{cut} range of 3-5kpc to be appropriate. Results are given in table 2. Assuming $h_{\text{cut}} = 3$ kpc, median P_{KS} are in the range $10^{-4} - 3 \times 10^{-2}$ for all models but L-I- \mathcal{A} and L-I- \mathcal{B} , meaning that the halo population is detected at least at a 97% confidence level. When $h_{\text{cut}} = 4$ kpc, numbers of

detected MSPs get smaller, but the cumulative distributions are even more distinct (see, e.g., the upper right panels of figure 7), resulting in $P_{\text{KS}} < 0.01$ for all models, i.e., in a detection confidence greater than 99%. P_{KS} values get again bigger for $h_{\text{cut}} = 5$ kpc (not shown in the table), because the extremely low number of detected MSPs undermines the effectiveness of the KS test. Notice that for some specific model we obtain $P_{\text{KS}} < 10^{-4}$, resulting in a detection confidence $> 99.99\%$; moreover, results are extremely encouraging even assuming the reduced SKA \mathcal{B} configuration. In all our tests we assumed an underlying disk population of 30000 MSPs. This number is somewhat uncertain, but the power of the KS test lies in the fact that it compares cumulative normalized distributions, which remain quite distinct even adding a substantial population of disk MSPs. Tests on models with 60000 disk MSPs give somewhat larger (factor of ≈ 2) P_{KS} , leaving our main results unchanged. We stress that in this analysis we considered all the disk MSPs, including those in binaries (the vast majority). If we restrict the disk sample to isolated MSPs, then the number of observable systems is expected to drop by a factor of four, making the halo population even more dominant at high h_{cut} . This, in turn, will strengthen our identification criterion.

6 CONCLUSIONS

Inspired by the detection of several MSPs in binaries in the core of Galactic GCs, we investigated their dynamical interaction with putative IMBHs lurking in the center of the same GCs. As a consequence of three body interactions, MSPs are ejected in the Galactic halo with velocities (with respect to the host GC) up to several hundreds km s^{-1} , sufficient to distribute them into the outer halo, but not to escape the Galaxy potential, allowing the formation of a substantial population of fast halo MSPs. The detection of such population would be a strong element, albeit indirect, in favor of the presence of IMBHs in the center of GCs.

We investigated four ejection scenarios, involving two different IMBH populations and MSPs formation histories. We considered a high -H- and a low -L- IMBH mass functions, consistent with the runaway model of Portegies Zwart et al. (2005) and with the low mass end extrapolation of the $M - \sigma$ relation respectively. We also assumed two different MSPs formation scenarios, one in which MSPs are simultaneously generated in a single burst 12Gyr ago, and one with a constant MSP formation rate along the whole Galaxy history. In both cases, the MSP population in GCs was normalized to match the observed numbers of MSPs in close binaries in the clusters Terzan 5 and 47 Tuc, and then scaled to all other GCs according to their structural parameters. The investigated scenarios predict between 100 and 600 fast MSPs wandering in the MW halo, a population that can in principle be detected with future radio surveys. We emphasize here that all the considered models are consistent with current MSP observations in GCs; that is, even considering efficient binary break-up and MSP ejection, GCs retain a substantial population of binaries containing MSPs, as observed today.

In the spirit of using fast halo MSPs as a probe of IMBHs in GCs, we checked that such population cannot result from alternative channels. Halo MSPs can be in princi-

ple produced by other dynamical ejection mechanisms, such as binary-binary or three body interaction with stellar BHs, or can be relics of the natural evolution of the old halo stellar population. Both channels looks inefficient in producing a sizable population of halo MSPs, unless several tens of stellar BHs are retained in GCs, or the MSP formation efficiency is much higher in the halo than in the disk.

We finally ran fully consistent simulations of the MSP population in the Galaxy. We considered 30000 MSPs distributed in the disk plus several fast halo MSP populations predicted by our models. The disk and the halo populations were averaged over 1000 and 20 realizations respectively. We simulated observations with SKA, taking into account for selection effects and limiting sensitivity of the instrument. We found the distribution of projected distances from the galactic plane h to be an effective discriminant between the two populations. Fast halo MSPs, in fact, show a significant excess of objects at high h , in sharp contrast with standard disk-born MSPs. This means that any excess of MSPs at high h would be a strong hint of the presence of a different MSP population. Here we showed that MSP ejection from GC, due to dynamical interactions with IMBHs, would easily produce such excess, and can therefore leave a clear imprint in future radio surveys. We quantified the statistical significance of halo MSP detection by performing tests on synthetic samples drawn from the disk plus halo distribution. Results shown in figure 7 and table 2 are very encouraging. If we isolate the distribution of MSPs observed at distances from the galactic plane larger than $h_{\text{cut}} = 3$ kpc, the halo population is, on average, detected at a 97% confidence level for all models but L-I-A and L-I-B. When $h_{\text{cut}} = 4$ kpc, detection confidence is boosted to better than 99% for all models. This is also true for the reduced SKA B configuration, indicating that such detection will be easily feasible.

Our analysis is admittedly oversimplified in several respects. Most importantly, the disk MSP population is hard to model, since ~ 100 objects has been detected to date. This introduces considerable uncertainties in our results. Note however that, unless disk MSPs are far more numerous than suggested by present observation or extend far above the MW disk height, our basic result, that an excess of MSPs located at large distances from the Galactic plane would strongly support dynamical ejection due to IMBH residing in GCs, remains unaltered.

ACKNOWLEDGMENTS

We thank the anonymous referee for the valuable feedback that led to a significant improvement of the manuscript. AS was supported by the DFG grant SFB/TR 7 "Gravitational Wave Astronomy". NS acknowledges the support of ASI/INAF through grant I/009/10/0. AP received support from the PRIN INAF 2010. AS also acknowledges Piero Madau, Francesco Haardt and Monica Colpi for early discussions and suggestions that led to the start of this project.

REFERENCES

Archibald A. M. et al., 2009, *Science*, 324, 1411

- Bacon D., Sigurdsson S. & Davies M. B., 1996, *MNRAS*, 281, 830
 Binney J. & Tremaine S., "Galactic dynamics", Princeton, NJ, Princeton University Press, 1987, 747 p.
 Bhattacharya D., & van den Heuvel E. P. J., 1991, *Physical Report*, 203, 1
 Baumgardt H., Hut P., Makino J., McMillan S. & Portegies Zwart S., 2003a, *ApJ*, 582, 21
 Baumgardt H., Makino J., Hut P., McMillan S. & Portegies Zwart S., 2003b, *ApJ*, 589, 25
 Baumgardt H., Makino J. & Hut P. 2005, *ApJ*, 620, 238
 Beccari G., Pasquato M., De Marchi G., Dalessandro E., Trenti M. & Gill M., 2010, *ApJ*, 713, 194
 Bell E. F. et al., 2008, *ApJ*, 680, 295
 Bromley B. C., Kenyon S. J., Geller M. J., Barcikowski E., Brown W. R. & Kurtz M. J., 2006, *ApJ*, 653, 1194
 Brown W. R., et. al. 2010, *AJ*, 139,59
 Camilo F., Lorimer D. R., Freire P. C., Lyne A. G., Manchester R. N., 2000, *ApJ*, 535, 975
 Camilo F & Rasio F. A. 2005, *ASPC*, 328, 147
 Chakrabarty D., 2006, *AJ*, 131, 2561
 Cordes, J. M., & Chernoff, D. F., 1997, *ApJ*, 482, 971
 Cseh D., Kaaret P., Corbel S., Krdring E., Coriat M., Tzioumis A. & Lanzoni, B., 2010, *MNRAS*, 406, 1049
 Devecchi, B., Colpi, M., Mapelli, M., & Possenti, A. 2007, *MNRAS*, 380, 691
 Faucher-Giguère C. A. & Loeb A., 2010, *JCAP*, 1, 5
 Gebhardt K., Rich R. M. & Ho L. C., 2002, *ApJ*, 578, 41
 Gebhardt K., Rich R. M. & Ho L. C., 2005, *ApJ*, 634, 1093
 Gillessen S., Eisenhauer F., Fritz T. K., Bartko H., Dodds-Eden K., Pfuhl O., Ott T. & Genzel R., 2009, *ApJ*, 707, 114
 Glebbeek E., Gaburov E., de Mink S. E., Pols O. R. & Portegies Zwart S. F., 2009, *A&A*, 497, 255
 Gonzalez, M. E., Stairs, I. H., Ferdman, R. D., et al. 2011, *ApJ*, 743, 102
 Harris W. E., 1996, *AJ*, 112, 1487
 Hills J. G., 1975, *AJ*, 80, 809
 Hills J. G., 1988, *Nature*, 331, 687
 Ibatova R. et al., 2009, *ApJ*, 699, 169
 Ivanova N., Heinke C. O., Rasio F. A., Belczynski K. & Fregeau, J. M., 2008a, *MNRAS*, 386, 553
 Ivanova N., Heinke C. O. & Rasio F. A., 2008b, *IAUS*, 246, 316
 King A. R., Davies M. B. & Beer M. E., 2003, *MNRAS*, 345, 678
 Kobayashi S., Hainick Y., Sari R. & Rossi E. M., 2012, *ApJ*, 748, 105
 Kramer M., Xilouris K. M., Lorimer D. R., Doroshenko O., Jessner A., Wielebinski R., Wolszczan A. & Camilo F., 1998, *ApJ*, 501, 270
 Lazio J., 2009, arXiv:0910:0632
 Lorimer D. R., 2005, *LRR*, 8, 7
 Lorimer D. R. et al., 2006, *MNRAS*, 372, 777
 Lorimer D. R., 2008, *LRR*, 11, 8
 Lyne A. G. et al., 1998, *MNRAS*, 295, 743
 Maccarone, T. J., & Servillat, M. 2008, *MNRAS*, 389, 379
 McConnell D., Deshpande A. A., Connors T. & Ables J. G., 2004, *MNRAS*, 348, 1409
 McLaughlin D. E., 2000, *ApJ*, 539, 618
 McLaughlin D. E., 2003, *Proceedings of the ESO Workshop Held in Garching, Germany, 27-30 August 2002, ESO ASTROPHYSICS SYMPOSIA*. ISBN 3-540-40472-4. Edited by M. Kissler-Patig. Springer-Verlag, 2003, p. 329
 McLaughlin D. E. & Fall S. M., 2008, *ApJ*, 679, 1272
 Miller M. C. & Hamilton D. P., 2002, *MNRAS*, 330, 232
 Muno M. P. et al., 2003, *ApJ*, 589, 225
 Noyola E., Gebhardt K. & Bergmann M., 2008, *ApJ*, 676, 1008
 Nucita A. A., de Paolis F., Ingresso G., Carpano S. & Guainazzi M., 2008, *A&A*, 478, 763
 O'Leary R. M., Rasio F. A., Fregeau J. M., Ivanova N. & O'Shaughnessy R., 2006, *ApJ*, 637, 937

- Pasquato M., Trenti M., De Marchi G., Gill M., Hamilton D. P., Miller M. C., Stiavelli M. & van der Marel R. P., 2009, *ApJ*, 699, 1511
- Pooley, D., et al. 2003, *ApJL*, 591, L131
- Portegies Zwart S. & McMillan S. L. W., 2002, *ApJ*, 576, 899
- Portegies Zwart S., Baumgardt H., Hut P., Makino J. & McMillan S. L. W., 2004, *Nature*, 428, 724
- Portegies Zwart S., 2005, n "Joint Evolution of Black Holes and Galaxies" of the Series in High Energy Physics, Cosmology and Gravitation. IOP Publishing, Bristol and Philadelphia, 2005, eds M. Colpi, V.Gorini, F.Haardt and U.Moschella
- Sari R., Kobayashi S. & Rossi E. M., 2010, *ApJ*, 708, 605
- Sartore N., et al. 2010, *A&A*, 510, 23
- Sesana A., Haardt F. & Madau P., 2007, *MNRAS*, 379, 45
- Smits R., et al. 2009, *A&A*, 490, 1161
- Smits R., Tingay S. J., Wex N., Kramer M. & Stappers B., 2011, *A&A*, 528, 108
- Sollima A., Bellazzini M., Smart R. L., Correnti M., Pancino E., Ferraro F. R. & Romano D., 2009, *MNRAS*, 396, 2183
- Story, S. A., Gonthier, P. L., & Harding, A. K. 2007, *ApJ*, 671, 713
- Tremaine S. et al., 2002, *ApJ*, 574, 740
- Trenti M., 2008, *IAUS*, 246, 256
- Umbreit S., Fregeau J. M. & Rasio F. A., 2009, arXiv:0910.5293
- van den Bosch R., de Zeeuw T., Gebhardt K., Noyola E. & van de Ven G., 2006, *ApJ*, 641, 852
- van den Heuvel E. P. J., 1995, *Journal of Astrophysics and Astronomy*, 16, 255
- van den Heuvel E. P. J. & van Paradijs J., 1988, *Nature*, 334, 227
- van der Marel R. P. & Anderson J., 2010, *ApJ*, 710, 1063